Effects of Static and Dynamic Load Models on Power System Load Representation

Pichai Aree
Department of Electrical Engineering, Faculty of Engineering,
Thammasat University, Phathumtani, 12121, Thailand.

Abstract

In this paper, the multi-machine power system model in [1,2] is extended to include a dynamic load model. The effects of using static and dynamic load models to represent the electrical load of the power system with a constant power type, i.e., an aggregate induction motor is fully investigated through small-signal analysis. The eigenvalue and participation factor techniques are used. The results obtained from 9-bus test power system reveal widely different ways of power system dynamic performances with the static and dynamic load models being used.

Keywords: Static and Dynamic Load models, Small-Signal Analysis.

1. Introduction

Over a number of years, close attention has always been given to modeling of generators and their associated controls in the study of power system stability [2-4]. Under situation of load growth, power systems tend to be operated near their maximum capacity limits. The need for modeling research has become apparent, as traditional power system models are not adequate to describe all events that occur under heavy load conditions [5]. As recent survey, an increase in system loading is often reflected as a decrease in the level of system damping. To obtain a very good estimation of remaining damping under heavy load condition, it is important to have a reliable load model to be included into the power system so that system planners and operators have confidence in results obtained from analysis tool. So load modeling is of the issues addressed in this paper.

Traditionally, in small-signal stability analysis power system loads have been simply represented by constant impedances [3,4,6]. In highly stressed area of power system, recent studies in [7,8] have shown that using the constant impedance representation in small-signal analysis tends to overestimate system damping by about 25 % as compared with a more accurate load representation. To obtain more accurate damping assessment the static voltage-dependent load model in [2,9] has been incorporated into the dynamic model of multi-machine power system. The assessments of system damping with different types of the static voltage-dependent load models were conducted. The results showed the voltage-dependent load model has a great influence on damping of power system over the constant impedance load representation, when high loadability of the constant power or MVA type of power system load was considered. Since the majority of large industrial loads in power systems are constant power type, i.e., induction motors, their dynamic responses play a key role in the transient behavior of the entire system [10,11]. The application of the static voltage-dependent load model to represent them may be inadequate due to neglecting their dynamic natures [7]. So, the dynamic load model may need to be incorporated into the multi-machine power system with fundamental tread-off between the accuracy and complexity.

Since the industrial plants are composed of a large number of induction motors, it is not realistic to model every induction motor that is in the system. So the aggregate models with minimum order are needed to represent a group of induction motors. Along the years, various methods have been proposed for handing with aggregation of induction motor models [12-14]. Among them, the methodology based on the steady state and the transient starting-up

approaches in [13], was selected in this paper for finding the equivalent of circuit and inertia of aggregate induction motors, respectively.

The paper is organized as follows. In section 2, the small-signal model of a multi-machine power system with the static voltage-dependent and dynamic load models is addressed. The structure model of n-bus m-machine power system presented in [1,2] is extended to include the dynamic representation of aggregate induction motor load. Because traditional variables of induction motor in the orthogonal system (direct- and quadrature-axes) lack physical significance in the power system study, a new meaningful polar coordinate system is used to represent the motor's variables, i.e., bus voltage magnitude and angle. In section 3, 9-bus test power system is presented. In section 4, the effects of the static and dynamic load models on small-signal dynamic performances are fully investigated.

2. Power System Modeling

2.1 Multi-machine power system model

A multi-machine power system may be modeled in the form,

$$\dot{x} = f(x, y, p) \tag{1}$$

$$0 = g(x, y, p) \tag{2}$$

where, x is the state variable, y is an algebraic variable, p is the parameter vector.

Following along the technique presented in [1,2], the comprehensive small-signal stability model of m-machine n-bus power system in linearized form about the operating points in (1) and (2) are rewritten in matrix form as,

$$\begin{bmatrix} \Delta\dot{X}_g \\ 0 \end{bmatrix} = \begin{bmatrix} A & B \\ C & D \end{bmatrix} \begin{bmatrix} \Delta X_g \\ \Delta V \end{bmatrix} + \begin{bmatrix} 0 \\ \Delta S_L^{stat} \end{bmatrix} + \begin{bmatrix} 0 \\ \Delta S_L^{dyna} \end{bmatrix} + \begin{bmatrix} E_g \\ 0 \end{bmatrix} \Delta U_g \tag{3}$$

where, $\Delta X_g = [\Delta X_1, \Delta X_i, ..., \Delta X_m]^T$ (4)

$$\Delta V = \begin{bmatrix} \Delta V_g & \Delta V_\ell \end{bmatrix}^T \tag{5}$$

$$\Delta S_L^{stat} = \begin{bmatrix} \Delta S_{Lg}^{stat} & \Delta S_{L\ell}^{stat} \end{bmatrix}^T \tag{6}$$

$$\Delta S_L^{dyna} = \begin{bmatrix} \Delta S_{Lg}^{dyna} & \Delta S_{L\ell}^{dyna} \end{bmatrix}^T \tag{7}$$

$$\Delta X_i = [\Delta\delta_i \ \Delta\omega_i \ \Delta E'_{di} \ \Delta E'_{qi} \ \Delta E_{fi} \ \Delta V_{Ri} \ \Delta R_{Fi}]^T \tag{8}$$

In (3), the generators are modeled with field winding and one damper winding in q-axis. The generators are equipped with the IEEE type-1 excitation system. The lists of 7-state variables for i^{th} generator and its excitation system are given in (8). More details in matrix structure in (3) are documented in [2]. It should be noted that the subscript Lg and $L\ell$ stand for electrical load in connection with the PV and PQ buses, and superscript $stat$ and $dyna$ stand for static and dynamic loads, respectively.

2.2 Static Voltage-Dependent Load model

The static voltage-dependent load model is traditionally represented in an exponential form. For i^{th} load bus, injected electrical power is given in matrix form by

$$S_{L,i}^{stat} = \begin{bmatrix} -P_{L,i}^{stat} & -Q_{L,i}^{stat} \end{bmatrix}^T \tag{9}$$

where, $P_{L,i}^{stat} = P_{L,i}^0 \left(V_i / V_i^0 \right)^{npi}$ (10)

$$Q_{L,i}^{stat} = Q_{L,i}^0 \left(V_i / V_i^0 \right)^{nqi} \tag{11}$$

$P_{L,i}^0$ and V_i^0 are, respectively, active power and nominal voltage of the i^{th} load bus. n_p and n_q are static voltage exponents of active and reactive powers. $n_p = n_q = 0$ yields constant power case, $n_p = n_q = 1$ the constant current case and $n_p = n_q = 2$, the constant impedance case. Linearizing (9) around the operating point, the block diagonal matrix H of static load model is obtained as,

$$\Delta S_L^{stat} = H \Delta V \tag{12}$$

where, $H = Diag(H_i)$ (13)

$$H_i = \begin{bmatrix} \partial P_{L,i}^{stat} / \partial\theta_i & \partial P_{L,i}^{stat} / \partial V_i \\ \partial Q_{L,i}^{stat} / \partial\theta_i & \partial Q_{L,i}^{stat} / \partial V_i \end{bmatrix} \tag{14}$$

2.3 Dynamic Load Model

The aggregate induction motor is considered as nonlinear dynamic load. The differential and algebraic equations governing 3rd-order model, well suited for stability studies [3,10], are,

$$\frac{dE'_Q}{dt} = -\omega_s s E'_D - \frac{1}{\tau'_{mo}} \left(E'_Q - (X_s - X') I_D \right) \tag{15}$$

$$\frac{dE'_D}{dt} = \omega_s s E'_Q - \frac{1}{\tau'_{mo}}\left(E'_D + (X_s - X')I_Q\right) \quad (16)$$

$$\frac{ds}{dt} = \frac{1}{2H_m}\left(T_m^0(1-s)^n - E'_Q I_Q - E'_D I_D\right) \quad (17)$$

$$V_D = E'_D - X' I_{Qs} + R_s I_D \quad (18)$$

$$V_Q = E'_Q + X' I_D + R_s I_Q \quad (19)$$

E'_Q and E'_D are, respectively, the direct (D) and quadrature (Q) voltages behind the transient reactance X'. τ'_{mo} is the rotor open-circuit time constant of motor. Because the dynamic equations of induction motor represented by the traditional orthogonal coordinate system (D and Q-axis) is not suitable to make clear the relationship between voltage and/or frequency and dynamic of power supplied to the machine, they are newly derived in the polar coordinate variables E', θ', V and θ by using the following relationships

$$E' = \sqrt{E'^2_D + E'^2_Q} \quad (20)$$

$$\theta' = \tan^{-1}\left(E'_D / E'_Q\right) \quad (21)$$

where E' and θ' represents transient *e.m.f.* and angle behind the transient reactance X'. V and θ are voltage and angle of i^{th} motor load bus.

Differentiating (20) and (21), we have,

$$E'^2 d\theta = E'_Q dE'_D + E'_D dE'_Q \quad (22)$$

$$E' dE' = E'_D dE'_D + E'_Q dE'_Q \quad (23)$$

Re-arranging (22) and (23) by making use of (15)-(19), then (24)-(26) in the polar form are obtained. The injected active and reactive powers for the i^{th} motor load bus expressed in the polar form can be seen by (27)-(29).

$$\frac{dE'_i}{dt} = -\left(\frac{1}{\tau'_{moi}} + \frac{(X_{Si} - X'_i)X'_i}{\tau'_{moi} Z_{Si}^2}\right)E'_i + \frac{(X_{Si} - X'_i)}{\tau'_{moi} Z_{Si}^2}\left(X'_i \cos(\theta_i - \theta'_i) - R_{Si}\sin(\theta_i - \theta'_i)\right)V_i \quad (24)$$

$$\frac{d\theta'_i}{dt} = -\omega_s s - \frac{(X_{Si} - X'_i)R_{Si}}{\tau'_{moi} Z_{Si}^2} + \frac{(X_{Si} - X'_i)\left(X'_i \sin(\theta_i - \theta'_i) + R_{Si}\cos(\theta_i - \theta'_i)\right)V_i}{\tau'_{moi} Z_{Si}^2 E'_i} \quad (25)$$

$$\frac{ds_i}{dt} = -\frac{1}{2H_{mi}}\left(\frac{-R_{Si}E'^2_i + \left(R_{Si}\cos(\theta_i - \theta'_i) + X'_i \sin(\theta_i - \theta'_i)\right)E'_i V_i}{Z_{Si}^2}\right) + \frac{1}{2H_{mi}}T_m^0(1-s)^n \quad (26)$$

$$0 = \frac{R_{Si}}{Z_{Si}^2}V_i E'_i \cos(\theta_i - \theta'_i) - \frac{X'_i}{Z_{Si}^2}V_i E'_i \sin(\theta_i - \theta'_i) - \frac{R_{Si}}{Z_{Si}^2}V_i^2 + P_i \quad (27)$$

$$0 = \frac{R_{Si}}{Z_{Si}^2}V_i E'_i \sin(\theta_i - \theta'_i) + \frac{X'_i}{Z_{Si}^2}V_i E'_i \cos(\theta_i - \theta'_i) - \frac{X'_i}{Z_{Si}^2}V_i^2 + Q_i \quad (28)$$

where, $Z_{Si} = \sqrt{R_{Si}^2 + X'^2_{Si}}$ (29)

For small perturbation, the differential and algebraic equations of induction motor load in (24-29) may be written in matrix from by,

$$\Delta\dot{X}_\ell = F1\Delta X_\ell + F2\Delta V + E_\ell \Delta U_\ell \quad (30)$$

$$0 = G1\Delta X_\ell + G2\Delta V + \Delta S_L^{dyna} \quad (31)$$

where, $\Delta X_\ell = [\Delta X_1, \Delta X_i, ..., \Delta X_n]^T$ (32)

$$\Delta X_i = \left[\Delta E'_i \ \Delta\theta'_i \ \Delta s_i\right]^T \quad (33)$$

2.4 Power System Model with Static and Dynamic Load Models

To study the influence of electrical load on small-signal dynamic performance, the static load model can be incorporated into m-machine n-bus power system by substituting (12) into (3), we have

$$\begin{bmatrix}\Delta\dot{X}_g \\ 0\end{bmatrix} = \begin{bmatrix}A & B \\ C & D+H\end{bmatrix}\begin{bmatrix}\Delta X_g \\ \Delta V\end{bmatrix} + \begin{bmatrix}0 \\ \Delta S_L^{dyna}\end{bmatrix} + \begin{bmatrix}E_g \\ 0\end{bmatrix}\Delta U_g \quad (34)$$

$$\begin{bmatrix} \Delta\dot{X}_g \\ 0 \\ 0 \\ \Delta\dot{X}_\ell \end{bmatrix} = \begin{bmatrix} A & B & 0 & 0 \\ C & D+H & I & 0 \\ 0 & G2 & I & G1 \\ 0 & F2 & 0 & F1 \end{bmatrix} \begin{bmatrix} \Delta X_g \\ \Delta V \\ \Delta S_L^{dyna} \\ \Delta X_\ell \end{bmatrix} + \begin{bmatrix} E_g & 0 \\ 0 & 0 \\ 0 & 0 \\ 0 & E_\ell \end{bmatrix} \begin{bmatrix} \Delta U_g \\ \Delta U_\ell \end{bmatrix} \tag{35}$$

After eliminating all load bus by keeping the buses in which are connected by the aggregate induction motor loads, the power system model including both static and dynamic load models may be written in matrix form in (35). Next eliminating all voltage and power algebraic variables, the comprehensive power system model including generators, their controllers, static and dynamic load models are obtained by,

$$\begin{bmatrix} \Delta\dot{X}_g \\ \Delta\dot{X}_\ell \end{bmatrix} = \begin{bmatrix} \bar{A} & \bar{B} \\ \bar{C} & \bar{D} \end{bmatrix} \begin{bmatrix} \Delta X_g \\ \Delta X_\ell \end{bmatrix} + \begin{bmatrix} E_g & 0 \\ 0 & E_\ell \end{bmatrix} \begin{bmatrix} \Delta U_g \\ \Delta U_\ell \end{bmatrix} \tag{36}$$

3. System under Study

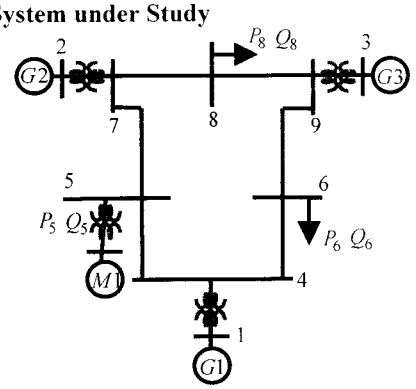

Fig. 1 9-bus test power system

The studies were conducted on 9-bus test power system as shown in Fig. 1. The overall form of model was that of the WSCC system in [6] except that a group of 2250-HP aggregate induction motors was connected to bus-5 via the step-down transformer. Three synchronous generators were equipped with the IEEE Type-1 excitation system. The generator and network parameters are available in [6], also 2250-hp induction motor parameters are given in [15-16]. For the case where the dynamic load model was considered, the equivalent circuit and parameters of aggregate induction motor load were calculated by using the technique presented in [13].

4. Static Versus Dynamic Load Models

In this section, the effects of the static and dynamic load models, used to represent a constant power type of electrical power system load, i.e., aggregate induction motor, were investigated. To make clear the fundamental effects of the static and dynamic load models on small-signal dynamic performances, all PQ load buses of the WSCC 9-bus system except bus-5 were assumed with the constant impedance representation. The components n_p and n_q of the static voltage-dependent load model were set to zero in corresponding to the constant power type of electrical load. The stable and unstable regions of the WSCC power system as increasing active power demand at bus-5 were investigated by observing the eigenvalues of the linearized power system model in (36).

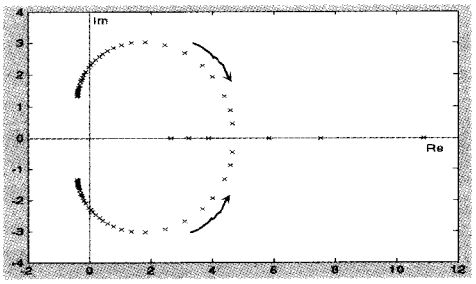

Fig. 2. Movement of critical eigenvalues as increasing in the electrical load demand at bus-5 for the case of static load model

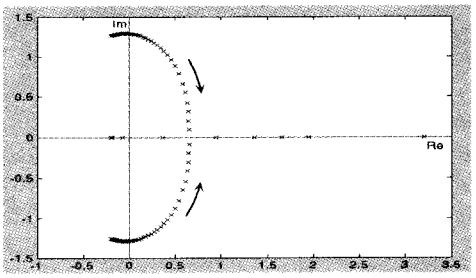

Fig. 3. Movement of critical eigenvalues as increasing in the electrical load demand at bus-5 for the case of dynamic load model

As a function of increasing electrical demand consumed by the bus-5 motor load, the movements of a complex pair of the critical eigenvalues crossing over into the right half plane were plotted as shown in Fig. 2 and 3. By making comparison, it is clearly seen that the critical eigenvalues of the system between using the static and dynamic load models cross the $j\omega$ axis in different locations. These critical eigenvalues are also given in Table 1, which were marked with the asterisk signs. It can be seen that large discrepancies in the magnitude of the critical eigenvalues are clearly observed with the different models of load representation. On continued increase in the electrical load demand, the complex pair of the unstable critical eigenvalues in Fig. 2 and 3 splits into real ones. One moves into the left-haft plane direction along the real axis. Another real eigenvalue moves into the right-half plane and returns to the left-half plane on the further increasing loads. So the system becomes stable again before it will experience the voltage instability at maximum loading point [17].

With static load model		With dynamic load model	
Load power demand at bus 5 $P_{L5}=3.24$ *p.u.* $Q_{L5}=1.23$ *p.u.*		Load power demand at bus 5 $P_{L5}=2.91$ *p.u.* $Q_{L5}=1.11$ *p.u.*	
Eigenvalues	Damping	Eigenvalues	Damping
-0.0000	1.00e+000	-0.0000	1.00e+000
-0.1973	1.00e+000	-0.1864	1.00e+000
-0.4413 - 0.5977i	5.94e-001	-0.4075 - 0.5708i	5.81e-001
-0.4413 + 0.5977i	5.94e-001	-0.4075 + 0.5708i	5.81e-001
-0.4008 - 0.7756i	4.59e-001	-0.3853 - 0.7615i	4.51e-001
-0.4008 + 0.7756i	4.59e-001	-0.3853 + 0.7615i	4.51e-001
0.0000 - 2.2517i *	-1.73e-005	0.0000 - 1.2875i *	-2.97e-005
0.0000 + 2.2517i *	-1.73e-005	0.0000 + 1.2875i *	-2.97e-005
-2.5057	1.00e+000	-1.4636	1.00e+000
-3.5964	1.00e+000	-3.4698	1.00e+000
-5.3965	1.00e+000	-4.7978	1.00e+000
-0.5634 - 8.1883i	6.86e-002	-6.0078	1.00e+000
-0.5634 + 8.1883i	6.86e-002	-0.4823 - 8.3566i	5.76e-002
-5.1803 - 9.5133i	4.78e-001	-0.4823 + 8.3566i	5.76e-002
-5.1803 + 9.5133i	4.78e-001	-5.2951 - 9.8248i	4.74e-001
-5.3474 - 9.8763i	4.76e-001	-5.2951 + 9.8248i	4.74e-001
-5.3474 + 9.8763i	4.76e-001	-5.3342 - 9.8801i	4.75e-001
-5.4845 - 9.8908i	4.85e-001	-5.3342 + 9.8801i	4.75e-001
-5.4845 + 9.8908i	4.85e-001	-5.4508 - 9.8928i	4.83e-001
-1.3720 -12.9662i	1.05e-001	-5.4508 + 9.8928i	4.83e-001
-1.3720 +12.9662i	1.05e-001	-1.2991 -12.9831i	9.96e-002
		-1.2991 +12.9831i	9.96e-002
		-4.8289 -19.5367i	2.40e-001
		-4.8289 +19.5367i	2.40e-001

Table 1. All eigenvalues and their damping ratios of 9-bus power system with the static (n_p= n_q=0) and dynamic load models

Table 1 shows all eigenvalues of the system and their damping ratios, when the bus-5's active (P) and reactive (Q) powers were increased until the system reached the critical point. This point is so-called Hopf bifurcation point (see in [17]), where a pair of the critical eigenvalues lies on the imaginary axis in the complex plane. On increase in the bus-5's electrical load demand, the power system with both static and dynamic load models experienced the small-signal instability through the subcritical Hopf bifurcation. However, Table 1 clearly indicates that the system became unstable with different amounts of active power consumed by the electrical load (3.24 and 2.91 per unit for the cases of static and dynamic load models, respectively). By making comparison, the 0.33 per-unit difference of active power indicates that using the static load model could yield optimistic results in the predictions of the

remaining margin of loadability and damping of the system before experiencing the subcritical Hopf bifurcation. It can be concluded that the dynamic load model has such a great influence on the small-signal dynamic performance and on accurate prediction of system damping.

The critical unstable eigenvalues between using static and dynamic load representations were further investigated by looking at the associated power system states, responsible for the critical unstable mode. A sensitivity analysis using participation factors in [18] was employed. The participation factors were normalized so their largest magnitudes were equal to one. They were plotted in Fig. 4 and 5 for the case of the static and dynamic load representations, respectively. On increasing electrical load demand at bus-5, Fig. 4 obviously shows that the critical unstable eigenvalues of system with the static load model are mainly due to the state variable $\Delta E'_q$ and ΔR_F pairs of generator G1, G2 and G3. This implies the dynamic interactions occur among the synchronous generators through the critical mode, causing the small-signal instability. As shown in Table 1, this mode is characterized by the oscillation mode with frequency of 2.2517 rad/s. For the case of the dynamic load model, Fig. 5 indicates that the critical unstable eigenvalues are strongly related to the generator (G1) and motor (M1) flux linkage pair ($\Delta E'_{q1}$ and $\Delta E'_1$) and also $\Delta E'_{q1}$ and ΔR_{F1} pair of generator G1. The rotor transients of generator and induction motor load play the dominant effect in exchanging their electromagnetic energies and mainly contribute to the unstable inter-area mode with the frequency of 1.2875 rad/s. It can be said that the static and dynamic load models interact with the generators in widely different manners via the critical oscillatory mode.

5. Conclusion

In this paper, the *m*-machine *n*-bus power system has been extended to include the dynamic model of aggregate induction motor load in the polar coordinate. The effects of the dynamic and static load models, representing the constant power type of electrical load, i.e., induction motor, have been fully investigated via small-signal analysis. Based on the results obtained, the dynamic load model has shown a tremendous effect on the small-signal dynamic performance. Using the dynamic load model is more realistic than using the static load model. Because the static load model would not be capable of capturing the true unstable dynamic behavior, using them may lead to misjudgement. Therefore, for the small-signal stability analysis, dynamic load models may need to be incorporated into the power system for representing the constant power type of electrical load such as induction motor. The dynamic load model could aid to capture a true dynamic behavior as well as a very good prediction of the remaining margins of loadability and damping before the system reaches the small-signal instability.

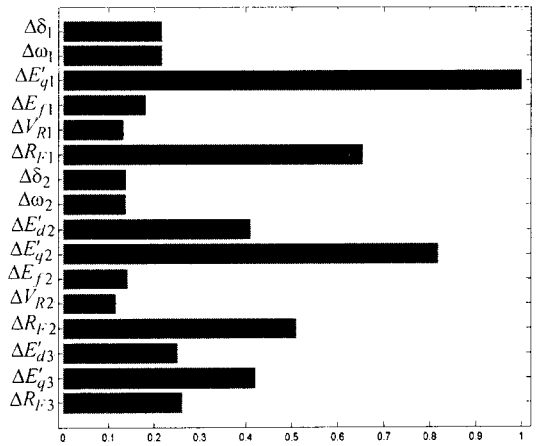

Fig. 4 Participation factors of critical eigenvalues for the case of static load model

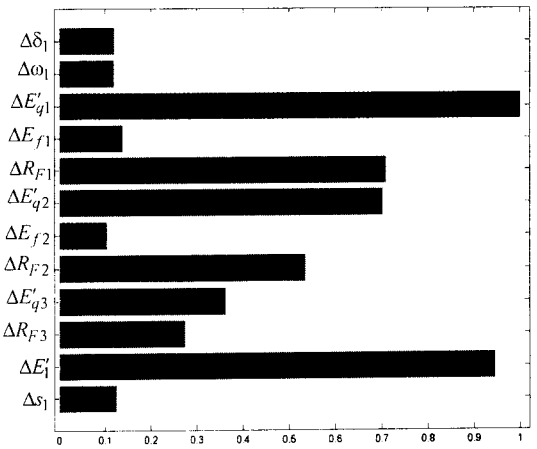

Fig. 5 Participation factors of critical eigenvalues for the case of dynamic load model

6. Acknowledgment

The results reported in this paper were carried out while P. Aree was on leave as visiting professor at the University of Alabama at Birmingham, Alabama, USA. Research salary support from the University of Alabama is gratefully acknowledged.

7. Reference

[1] Sauer, P. W. and Pai, M. A., Power System Steady-state and the Load Flow Jacobian, IEEE Transactions on Power Systems, Vol. 5, No. 4, pp. 1374-1383, 1990.

[2] Sauer, P. W., Pai, M. A., *Power System Dynamic and Stability*, Prentice-Hall, 1998.

[3] Kundur, P., *Power System Stability and Control*, McGraw-Hill, 1993.

[4] Padiyar, K. R., *Power System Dynamics Stability and Control*, John Wiley & Sons, 1995.

[5] Milanovic, J. V. and Hiskens, I. A., Effect of Load Dynamics on Power System Damping, IEEE Transactions on Power Systems, Vol. 10, No. 2, pp. 1022-1027, 1995.

[6] Anderson, P. M. and Fouad, A. A., *Power System Control and Stability*, Iowa State University Press, Ames, 1977.

[7] IEEE Committee Report, Load Representation for Dynamic Performance Analysis, IEEE Transactions on Power Systems, Vol. 2, No. 8, pp. 472-481, 1993.

[8] Moansour, Y., Application of Eigenanalysis to the Western North American Power System, IEEE Publication 90TH0292-3, Eigenanalysis and Frequency Domain Methods for Power System Dynamic Performance, 1990.

[9] Ranjan, R. K., Pai, M. A. and Sauer, P. W., Analytical Formulation of Small Signal Stability Analysis in Power System with Nonlinear Load Model, Indian Academy of Sciences, Bangalore, India, Journal of Engineering Sciences, Vol. 8, Part 5, pp. 869-889, 1993.

[10]Brereton, D. S., Lewis, D. G. and Young, C. C., Representation of Induction-Motor Loads During Power-System Stability Studies, AIEE Transactions, Vol. 76, pp. 451-461, 1957.

[11]Rogers, G. J., Manno, J. D. and Alden, R. T. H., An Aggregate Induction Motor Model for Industrial Plants, IEEE Transactions on Power Apparatus and Systems, Vol. 103, No. 4, pp. 683-690, 1984.

[12]Nozari, F., Kankam, M. D., W. W. P Aggregation of Induction Machines for Transient Stability Load Modeling, IEEE Transactions on Power System, Vol. 2, No. 4, pp. 1096-1103, 1987.

[13]Franklin, D. C. and Morelato, A., Improving Dynamic Aggregation of Induction Motor Models, IEEE Transactions on Power System, Vol. 9, No. 4, pp. 1934-1941, 1994.

[14]Taleb, M., Akbaba, M. and Abdullah, E. A., Aggregation of Induction Machines for Power System Dynamic Studies, IEEE Transactions on Power Systems, Vol. 9, No. 4, pp. 2042-2048, 1994.

[15]Cathey, J. J., Cavin, R. K., and Ayoub, A. K., Transient Load Model of an Induction Motor, IEEE Transactions on Power Apparatus and Systems, Vol. 92, No. 4, pp. 1399-1406, 1973.

[16]Krause, P. C., *Analysis of Electrical Machinery*, McGraw-Hill, 1986.

[17]Rajagopalan, C., Lesieutre, B., Sauer, P. W., and Pai, M. A., Dynamic Aspects of Voltage/Power Charactersitics, IEEE Transactions on Power Systems, Vol. 7, No. 3, pp. 990-1000, 1992.

[18]Verghese, G. C., Perez-Arriaga, I. J. and Scheweppe, F. C., Slective Model Analysis with Application to Electric Power System, IEEE Transactions on Power and Apparatus Systems, Vol. 101, No. 9, pp. 3117-3134, 1982.

Pichai Aree received his M.S.C. degree in electrical power engineering from the University of Manchester Institute Science and Technology (UMIST), England, in 1996, and P.h.D. degree in electrical engineering from the University of Glasgow, Scotland, in 2000. He joined Department of Electrical Engineering, Thammasat University (TU) in 1993. From June 2001 to May 2002, he was a visiting professor at the University of Alabama, at Birmingham, USA. He is currently a lecturer at Department of Electrical Engineering, TU. His research interests are power system dynamics, stability, and control.